

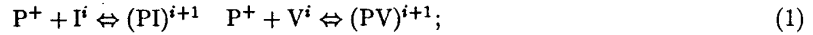
Consistent Quantitative Models for the Coupled Diffusion of Dopants and Point Defects in Silicon

S. T. Dunham

Department of Electrical, Computer and Systems Engineering,
Boston University, Boston, MA 02215

Substitutional dopants in silicon diffuse via point defects (interstitials and vacancies). Since the diffusion of phosphorus at high concentrations has long been considered "anomalous," we focus on phosphorus as the most challenging test case. Using a general model for the coupled diffusion of dopants and point defects, simplified by assumptions which we have shown to be appropriate, we present simulations of the coupled system to demonstrate that phosphorus diffusion profiles can be modeled quantitatively over the full range of doping levels from intrinsic to solid solubility using activated parameters which are consistent with the broad range of point defect and dopant diffusion phenomena. We use further simulations to illustrate how the diffusion behavior of the commonly-used dopants (As, B, P and Sb) arises from differences in the relative importance of interstitial and vacancy interactions, the magnitude of the effective dopant diffusivity and the location of defect ionization levels within the bandgap.

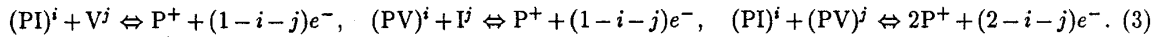
The system in which a dopant diffuses via interactions with point defects can be described by a set of reactions, including dopant/defect pairing reactions (i represents the charge state of the defect or pair):



Frenkel pair recombination/generation:



and reaction of pairs with the opposite type defect or pair (defect-mediated recombination):



There are also ionization or charge exchange reactions for each of the charged species. Because electronic interactions are much faster than the atomic diffusion processes, we assume that all ionization reactions are near equilibrium. Thus, for example, the concentrations of interstitials in the various charge states are given by $C_{I^i} \cong K_I^i (n_i/n)^i C_{I^0}$. We assume that there is local charge neutrality and complete impurity ionization (concentrations of charged defects and pairs are assumed negligible). We also ignore band-gap narrowing effects and use Boltzmann statistics. Based on this set of reactions and assumptions, we can write five continuity equations for the diffusion and reaction of substitutional dopants, interstitials, vacancies, dopant/interstitial pairs and dopant/vacancy pairs. The full set of equations is described in Reference [1].

There are a couple of other simplifying assumptions which have been commonly made in the literature. First, it is often assumed that the dopant/defect pairing reactions are near equilibrium [2-7], which implies that

$$C_{(PI)^{i+1}} \cong K_{P/I}^i C_P + C_{I^i} \cong K_{P/I}^i K_I^i \left(\frac{n_i}{n}\right)^i C_P + C_{I^0}, \quad (4)$$

where $K_{P/I}^i$ is the equilibrium constant for the pairing of dopant with interstitials in charge state i (Equation(1)). Another assumption sometimes used in modeling coupled diffusion is that the defect recombination reactions are also near equilibrium ($C_I C_V \cong C_I^* C_V^*$) [3, 6, 8, 9].

Using simulations of the full system described above, along with parameters based on previously reported experimental results, we can show that the assumption that the dopant/defect pairing reaction is near equilibrium is generally valid for high concentration phosphorus diffusion for times of interest for VLSI fabrication [1, 10], and therefore valid for all the major dopants, since phosphorus causes the largest disturbance of point defect concentrations from equilibrium. In contrast, even including dopant-mediated recombination and assuming no barrier to recombination, we find that the defect recombination process is *not* rapid enough to maintain local equilibrium between the defects (i.e., $C_I C_V \neq C_I^* C_V^*$). Since the dopant/defect pairing reaction is near equilibrium, we can reduce the number of differential equations and parameters needed to describe the system, solving just three continuity equations (for the dopant, interstitials and vacancies). The simulations shown in this work utilize this simplified model as implemented in a modified version of SUPREM IV [7].

Correctly modeling the changes in diffusion as a function of dose or surface concentrations is one of the most difficult challenges for high concentration diffusion modeling. We compare our models to an extensive set of experimental data reported by Yoshida *et al.* [11, 12] and Matsumoto and Niimi [13] at 900, 1000 and 1100°C, which include the full range of surface concentrations from intrinsic to solid-solubility. The phosphorus diffusivity

via positive, neutral and negative dopant/defect pairs in intrinsic material and the the effective rate of Frenkel pair recombination were determined by minimizing the difference between the simulated and measured profiles using a Levenberg-Marquardt optimization code (PROFILE [14]). The rest of the parameters, including all point defect parameters and intrinsic diffusivities are based on previously published experimental results (SUPREM IV defaults).

From measurement of enhanced and retard diffusion during nitridation of silicon and SiO₂, it has been concluded that in intrinsic material, phosphorus diffuses almost solely with interstitials [15]. If it is assumed that this remains true in extrinsic material as well, then diffusion via vacancies can be ignored. A similar model has been utilized in previous work [10, 16] to obtain a reasonable fit to a single profile by assuming rapid recombination, but these simulations significantly underestimated diffusion in the peak region.

The problem is much more severe when attempting to fit profiles over a range of peak concentrations. Figure 1 shows the best fit to the experimental data at 900°C considering diffusion via neutral and negatively-charged phosphorus/interstitial pairs, but neglecting diffusion via vacancies. From this plot, it is clear that without vacancies having an increased role at higher doping concentrations, the coupled diffusion model is unable to account for the experimental results over a range of doping levels. Similar behavior is observed at higher temperatures as well, further supporting this conclusion [1]. Note that since the effective recombination rate was optimized to match the data, very fast recombination is insufficient to produce the experimentally-observed high concentration diffusion profiles, in contrast to assertions made by Richardson and Mulvaney [17].

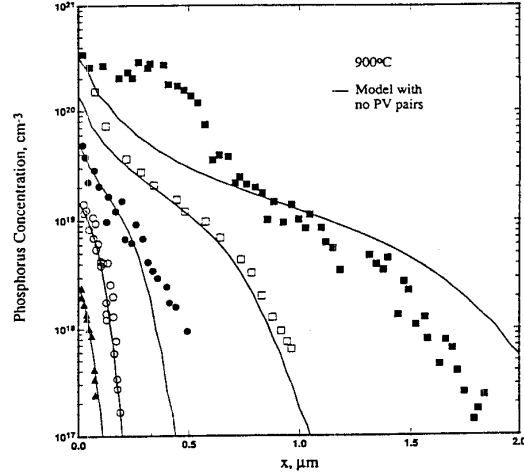


Figure 1: Active phosphorus concentration profiles based on simulations of 4h diffusions at 900°C neglecting diffusion via PV pairs. The data is as reported by Yoshida *et al.* [11, 12] and Matsumoto and Niimi [13].

Although observations of enhanced and retarded diffusion during oxidation and nitridation show that the diffusion of phosphorus in intrinsic material is dominated almost totally by interstitial mechanisms [15], the same is not necessarily true in heavily doped material. Phosphorus/vacancy pairs have been found to have an acceptor level well within the band gap [18]. Since the number of negatively-charged pairs increases in proportion to the square of the electron concentration, diffusion via negatively-charged vacancy pairs may be dominant near solid-solubility, while contributing less than 2% to diffusion in lightly-doped material. When diffusion via negatively-charged phosphorus/vacancy pairs is included, the coupled diffusion model does an excellent job of matching the experimental results over the full range of doping levels and temperatures. In our analysis, we constrain the phosphorus diffusion parameters and Frenkel pair recombination rate to have Arrhenius temperature dependences. Examples of the fit of the model to experimental data using activated parameters are shown in Figure 2 and the optimized parameters are listed in Table 1.

Table 1: Optimized temperature-activated parameters for phosphorus diffusion over the temperature range of 900-1100°C.

Parameter	Pre-Exponential Factor	Activation Energy
$D_{PI}^0 = D_{(PI)} + K_{P/I}^0 C_{I0}^*$	$4.8 \times 10^3 \text{ cm}^2/\text{s}$	4.51 eV
$D_{PI}^- = D_{(PI)} K_{P/I}^0 K_{PI}^- C_{I0}^*$	$3.1 \times 10^{-2} \text{ cm}^2/\text{s}$	3.20 eV
$D_{PV}^- = D_{(PV)} K_{P/V}^0 K_{PV}^- C_{V0}^*$	$3.6 \times 10^{-5} \text{ cm}^2/\text{s}$	2.90 eV
$k_{I/V}$	$1.9 \times 10^{-9} \text{ cm}^{-3} \text{ s}^{-1}$	1.23 eV

The lower activation energy calculated for diffusion via charged defects can be partially attributed to the Coulombic contribution to the dopant/defect binding energy. The calculated values for effective recombination rate are quite similar to the estimated diffusion-limited values, which implies that there is little or no barrier to Frenkel pair recombination, consistent with recent measurements based on enhanced and retarded diffusion during oxidation [19].

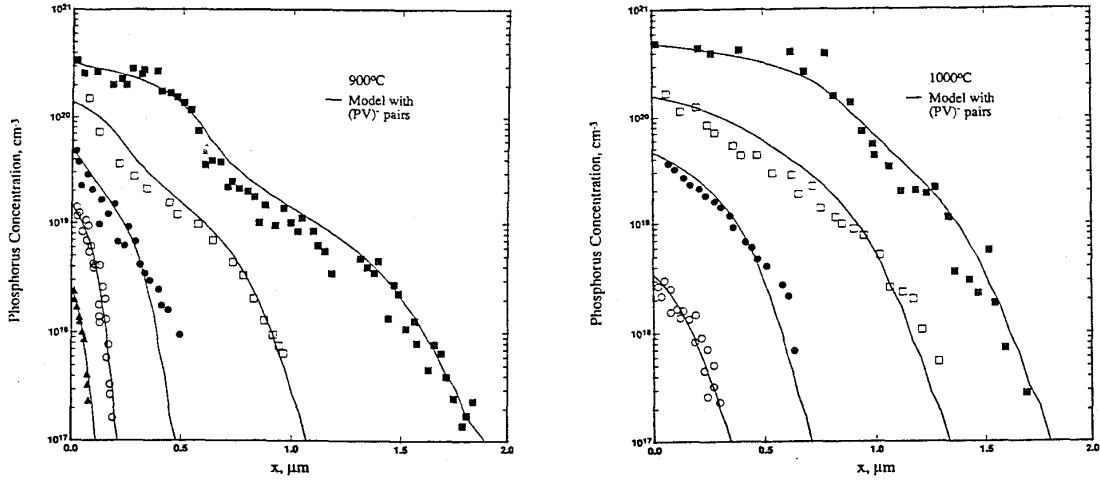


Figure 2: Active phosphorus concentration profiles based on simulations of diffusion at 900 and 1000°C, including diffusion via (PV)⁻ pairs. The data is as reported by Yoshida *et al.* [11, 12] and Matsumoto and Niimi [13].

We can also extend the coupled diffusion model to other dopants in order to understand why the different dopants manifest such different diffusion behavior. Antimony might be thought of as a direct analog to phosphorus since it diffuses almost solely via vacancy (versus interstitial) mechanisms. However, as shown in Figure 3, the coupled diffusion model correctly predicts that antimony will have box-like diffusion profiles with no significant enhanced tail diffusion.

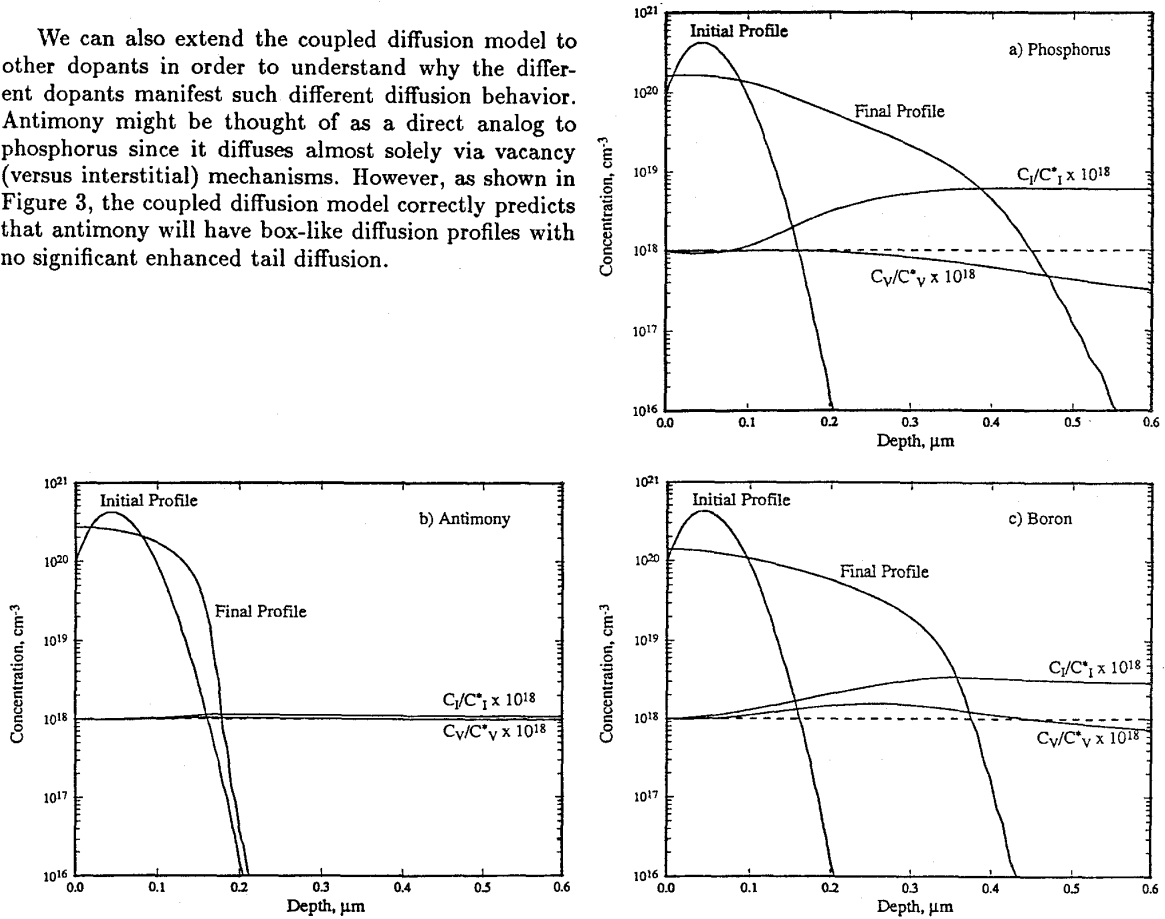


Figure 3: Simulated dopant and point defect concentration profiles for (a) phosphorus, (b) antimony and (c) boron following a 5 minute diffusion at 1000°C.

The differences between phosphorus and antimony profile shapes are mainly due to two factors. First, antimony diffuses much more slowly than phosphorus, so the flux of pairs into the bulk is much reduced and the point defect concentrations much less disturbed. Second, antimony diffuses primarily with vacancies and the equilibrium vacancy concentration is much greater than that for interstitials [20]. Thus, it is much harder to alter the vacancy concentration away from its equilibrium value. As expected, arsenic behaves similarly to antimony. The significant interstitial component of arsenic diffusion results in interstitial injection as well as vacancy injection into the bulk, with a small interstitial supersaturation possible under some conditions since $C_V^* \gg C_I^*$ (even though $f_I < 0.5$).

The source of the differences observed for antimony lead us to consider boron which, like phosphorus, diffuses rapidly and primarily with interstitials. However, when we apply the coupled diffusion model to boron, the resulting profile shapes are quite different, as shown in Figure 3. Simulated boron profiles lack the characteristic phosphorus kink and show less enhanced tail diffusion (as observed experimentally). These differences are primarily due to the fact that boron is an acceptor rather than a donor and the ionization states for the silicon interstitial favor positively rather than negatively charged defects [21]. Thus in *p*-type material (but much less so in *n*-type), the equilibrium interstitial concentration rises rapidly with doping. The higher equilibrium concentration makes the interstitial concentration more resistant to deviations from equilibrium, reducing the tail and eliminating the kink.

In summary, we have developed models for the coupled diffusion of dopants and point defects which can account quantitatively for phosphorus diffusion profiles over the full range of doping levels. By comparison to an extensive set of published experimental phosphorus diffusion profiles at 900, 1000 and 1100°C, we derived activated values for phosphorus diffusion parameters and Frenkel pair recombination. Extending the model to the other major dopants, we are able to predict the differences in profile shape that are observed experimentally.

This work was supported by a SEMATECH Center of Excellence grant #91-MC-503 and NSF grant #ECS-9009591.

References

- [1] S. T. Dunham, *J. Electrochem. Soc.* **139**, 2628 (1992).
- [2] D. Mathiot and J. C. Pfister, *J. Appl. Phys.* **55**, 3518 (1984).
- [3] F. F. Morehead and R. F. Lever, *Appl. Phys. Lett.* **48**, 151 (1986).
- [4] B. Mulvaney and W. Richardson, *Appl. Phys. Lett.* **51**, 1439 (1987).
- [5] M. Orłowski, *Appl. Phys. Lett.* **53**, 1323 (1988).
- [6] F. F. Morehead and R. F. Lever, *J. Appl. Phys.* **66**, 151 (1989).
- [7] M. E. Law and R. W. Dutton, *IEEE Trans. CAD* **7**, 181 (1988).
- [8] E. Rorris, R. R. O'Brien, F. F. Morehead, R. F. Lever, J. P. Peng and G. R. Srinivasan, *IEEE Trans. CAD* **9**, 1113 (1990).
- [9] D. Mathiot and S. Martin, *J. Appl. Phys.* **70**, 3071 (1991).
- [10] S. T. Dunham and R. A. Meade, in **Second International Symposium on Process Physics and Modeling in Semiconductor Technology**, G. Srinivasan, J. Plummer and S. Pantelides, eds. (Electrochem. Soc. Proc. **91-4**, Pennington, NJ, 1991) pp. 287-303.
- [11] M. Yoshida, *Jap. J. Appl. Phys.* **18**, 479 (1979).
- [12] M. Yoshida, E. Arai, H. Nakamura and Y. Terunuma, *J. Appl. Phys.* **45**, 1498 (1974).
- [13] S. Matsumoto and T. Niimi, *Jap. J. Appl. Phys.* **15**, 2077 (1976).
- [14] G. J. L. Ouwering, *The PROFILE/PROF2D User's Manual*, Delft University of Technology, 1987.
- [15] P. Fahey, G. Barbuscia, M. Moslehi and R. W. Dutton, *Appl. Phys. Lett.* **43**, 683 (1983).
- [16] W. Richardson and B. Mulvaney, *J. Appl. Phys.* **65**, 2243 (1989).
- [17] W. Richardson and B. Mulvaney, *Appl. Phys. Lett.* **53**, 1917 (1988).
- [18] L. C. Kimerling, *Inst. Phys. Conf. Ser.* **31**, 221 (1977).
- [19] E. Guerrero, W. Jüngling, H. Pötzl, U. Gösele, M. Grasserbauer and G. Stingeder, *J. Electrochem. Soc.* **133**, 2181 (1986).
- [20] T. Y. Tan and U. Gösele, *Appl. Phys.* **A37**, 1 (1985).
- [21] M. D. Giles, *IEEE Trans. CAD* **8**, 460 (1989).